

E. L. GUREVICH AND R. HERGENRÖDER  
ISAS—INSTITUTE FOR ANALYTICAL SCIENCES,  
BUNSEN-KIRCHHOFF-STRASSE, 11, 44139,  
DORTMUND, GERMANY

# Femtosecond Laser-Induced Breakdown Spectroscopy: Physics, Applications, and Perspectives

## INTRODUCTION

Progress in technology and society continually places new demands on analytical science and more powerful and informative methods need to be developed. One among them is laser-induced breakdown spectroscopy (LIBS), sometimes also referred to as LIPS (laser-induced plasma spectroscopy). Typically, LIBS measurements are conducted with nanosecond time scale lasers. A review by Song et al.<sup>1</sup> and two recently published books by Miziolek et al.<sup>2</sup> and Cremers et al.<sup>3</sup> give a good overview of instrumental developments in this area. However, new developments in laser technology have made ultra-short lasers available<sup>4</sup> and have stimulated an interest in LIBS with ultra-short pulses. There are fundamental differences between the ablation processes of

ultra-short ( $<1$  ps) and short ( $>1$  ps) pulses that result in different mechanisms of energy dissipation in the sample. In the case of ultra-short laser pulses, at the end of the laser pulse, only a very hot electron gas and a practically undisturbed lattice are found, which subsequently interact. However, for longer pulses above a certain energy threshold, the material undergoes transient changes in the thermodynamic states from solid, through liquid, into a plasma state.<sup>5,6</sup> Based on this difference, consequences for the analytical performance of the method can be expected that in the future should lead to new aspects in instrumentation and applications of LIBS. The goal of this review is to summarize current knowledge of the instrumentation and physics of laser ablation with femtosecond lasers and to draw some conclusions concerning new

possible applications that rely on these specific new features. It seems clear that even if a better performance in terms of analytical figures of merit compared to standard LIBS applications<sup>7</sup> is found, a replacement of current technology cannot be expected soon due to the cost and complexity of chirped pulse amplification (CPA) laser systems. However, current trends in other fields of application of these laser systems, e.g., medical laser applications or material processing,<sup>8</sup> may change this picture in the near future.

## PECULIARITIES OF FEMTOSECOND LASER-INDUCED BREAKDOWN SPECTROSCOPY SETUPS

As a starting point of the discussion, a typical fs-LIBS setup and its peculiarities compared to a standard setup are discussed. On first inspection

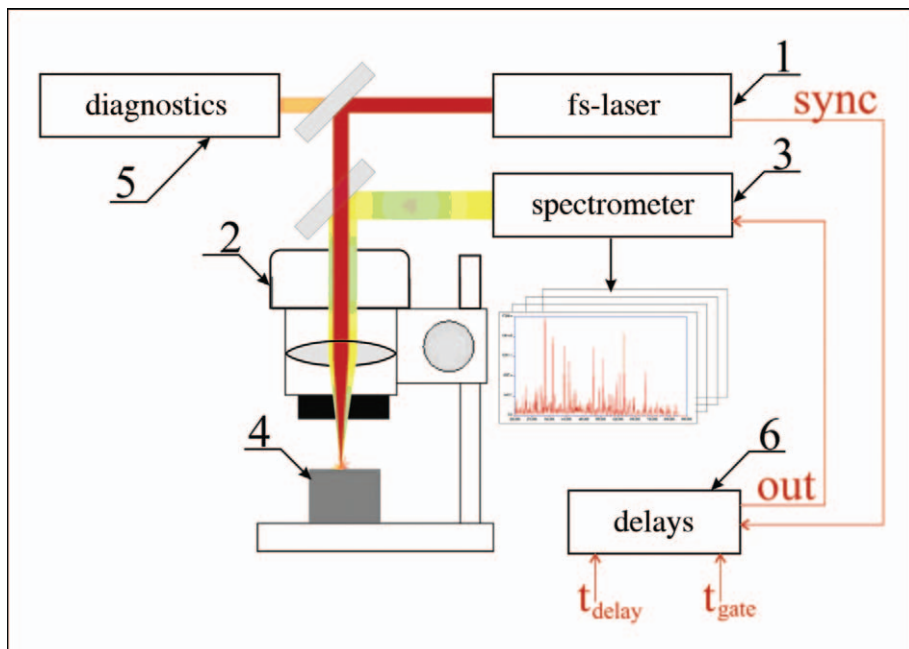


**Fig. 1. Schematic representation of a typical LIBS setup. (1) (Fs) laser generating strong electromagnetic pulses used for the ablation; (2) microscope; (3) optical spectrometer analyzing the light emitted by the plasma; (4) analyzed sample; (5) laser beam diagnostics; (6) delay generator for the spectrometer synchronization.**

tion not much difference can be seen from Fig. 1. The laser beam is focused by means of the optical setup (2) on the surface of a sample (4) or in the volume of gas to be analyzed. A conventional nanosecond or a femtosecond laser (1) can be used as the source. The laser radiation should be powerful enough to cause the ablation of the analyzed material.

If the laser irradiance is high enough, a plasma consisting of ablated material will appear. Part of the energy is used for sample heating and phase transition into the gaseous state; the excess of the incoming energy is transferred to the kinetic energy of the ablated species and to their excitation. De-excitation events are accompanied by characteristic light emission, which can be analyzed by an optical spectrometer (3). The emitted radiation is collected through the objective (2) used for the focusing of the laser radiation (as shown in the figure) or through a separate optical path.

Compared to conventional LIBS, for which basically only the laser energy is controlled, fs-LIBS needs

more diagnostics (5). Pulse duration, temporal pulse shape on the fs scale, and sometimes even the “chirp”, i.e., the distribution of the time-dependent carrier frequency over the pulse, have to be monitored. The pulse duration and temporal pulse shape are typically characterized by some intensity autocorrelation method<sup>4</sup> and a fast photodiode. The measurement of the chirp needs more sophisticated instrumentation that basically measures the spectrum of the pulse as a function of time. These techniques are known by acronyms such as “SPIDER”, “FROG”, etc. The necessity of these additional diagnostic tools will be discussed later.

The sampling time of the spectrometer (3) is defined by the delay generator (6), which is synchronized with the laser pulse. Experiments demonstrate a strong dependence of the signal-to-noise ratio and the detection limit on the delay and the gate times of the spectrometer. This still holds for fs-LIBS.<sup>9,10</sup>

The main difference of fs-LIBS with respect to conventional LIBS is obviously the use of a femtosecond

laser. The duration of the laser pulse has been continuously reduced since the invention of the laser. Systems with a pulse duration down to approximately 10 fs are now commercially available.

Commercially available femtosecond lasers are complicated systems basically consisting of three lasers. The principle layout can be found in Fig. 2. The concept of chirped pulse amplification (CPA) is central to these systems.<sup>4,11,12</sup> Femtosecond pulses are generated in the seeding laser, which is a mode-locked laser with an additional compression mechanism typically based on Kerr lens mode-locking.<sup>4</sup> The output is normally a train of fs pulses of extremely low pulse energy (pJ to nJ) and a repetition rate on the order of 10 MHz. Short pulses cannot be amplified efficiently, so they are temporally extended in the stretcher up to 0.1 to 1 ns. Here, the fact that a short, mode-locked pulse corresponds to a broad spectral width is used. The idea of the stretcher is illustrated in Fig. 3. Different spectral components propagate different distances in a tilted grating (or other dispersive element) configuration. As a result, “chirped” pulses are produced, in which different spectral components are temporally shifted relative to each other. Because linear amplification conserves the spectrum, the femtosecond pulse can be recompressed after amplification in a similar but reversed configuration.

In the next step, the stretched pulses are amplified. Nowadays, regenerative amplifiers are solely employed in this step.<sup>4</sup> After compression, the resulting pulses of commercially available systems are in the range of 20–200 fs with several mJ of energy, which corresponds to about 100 TW per cm<sup>2</sup> in a focused beam. Laboratory devices have reached the physical limit for CPA-based lasers of several femtoseconds. For reviews, see Refs. 4 and 12 and references therein.

However, from a practical point of view there is an upper energy limit for fs-LIBS, which currently can only be overcome with great effort.

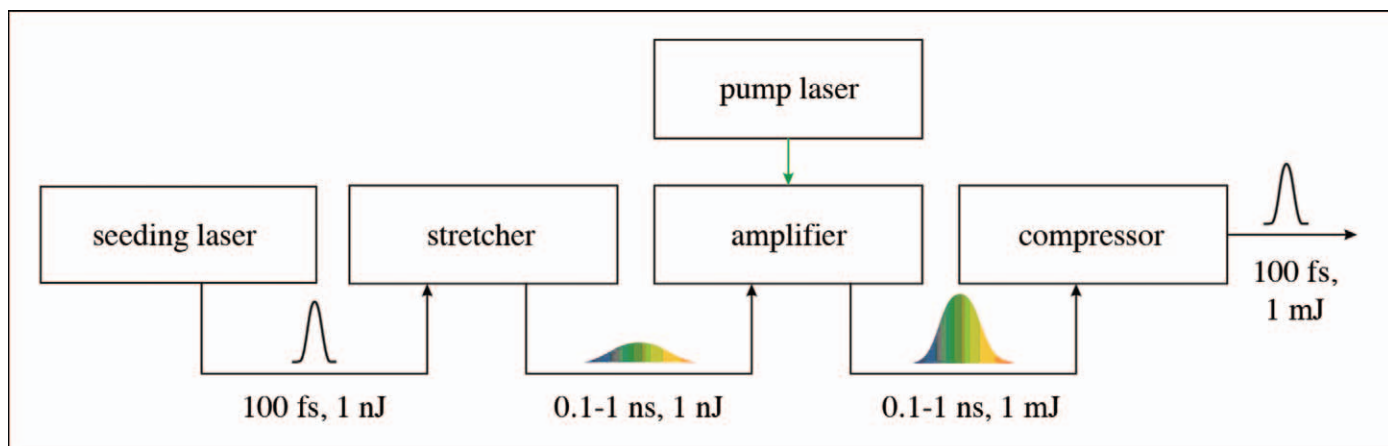


FIG. 2. Principles of the chirped pulse amplification.

It is provided by the efficiency of the output Pockels cell in the amplifier, which cuts single pulses out of the pulse train. Because there is an inherent leakage, a small part of the pulse is ejected out of the amplifier on each round trip of the pulse in the cavity. This pulse is then compressed and injected into the optical setup some nanoseconds before the main femtosecond pulse. Hence, it is referred to as *pre-pulse*. Normally, in a well-aligned system the pre-pulse amplitude is two to three orders of

magnitude smaller than the amplitude of the main pulse. However, if the laser energy is high enough, it may reach the ablation threshold or at least pre-heat or melt the sample.<sup>13</sup> In that case, the ablation scenario is completely changed and is much closer to conventional ns-laser ablation.

A non-optimal Pockels cell timing can also cause a post-pulse to appear several nanoseconds after the main pulse. This pulse can reheat the ablation plasma similar to ns-domain

and double-pulse LIBS experiments. The existence of additional pulses can be revealed by a fast photodiode, which cannot resolve the femtosecond pulses completely, but can indicate the existence of the pre- or the post-pulse (see Fig. 4).

The microscope (2) of the femtosecond LIBS setup (see Fig. 2) should be specially designed for ultra-short pulses. The typical value of the peak power of the beam is on the order of several tens of  $\text{GW}/\text{cm}^2$ , which puts high demands on the robustness of the optical components. At the focus, this corresponds to at least several  $\text{TW}/\text{cm}^2$ , which is far beyond the threshold for optical breakdown in air or glass. Hence, the only focal waist should be at the sample surface or even slightly beneath the surface. If there is another focus somewhere in front of the analyzed sample, the resulting optical breakdown will lead to a number of interesting physical effects such as plasma formation, self-focusing,<sup>14,15</sup> filamentation,<sup>16</sup> frequency shift, and broadening.<sup>17-19</sup> Most of these decrease the quality of the LIBS analysis because a part of the laser energy is consumed and the spatial and temporal characteristics are distorted. However, some of these mechanisms can be used beneficially for fs-LIBS (see, for example, Ref. 20).

The temporal characteristics of the ultra-short laser pulse may also be distorted through a misalignment or a tilt of the laser beam with respect

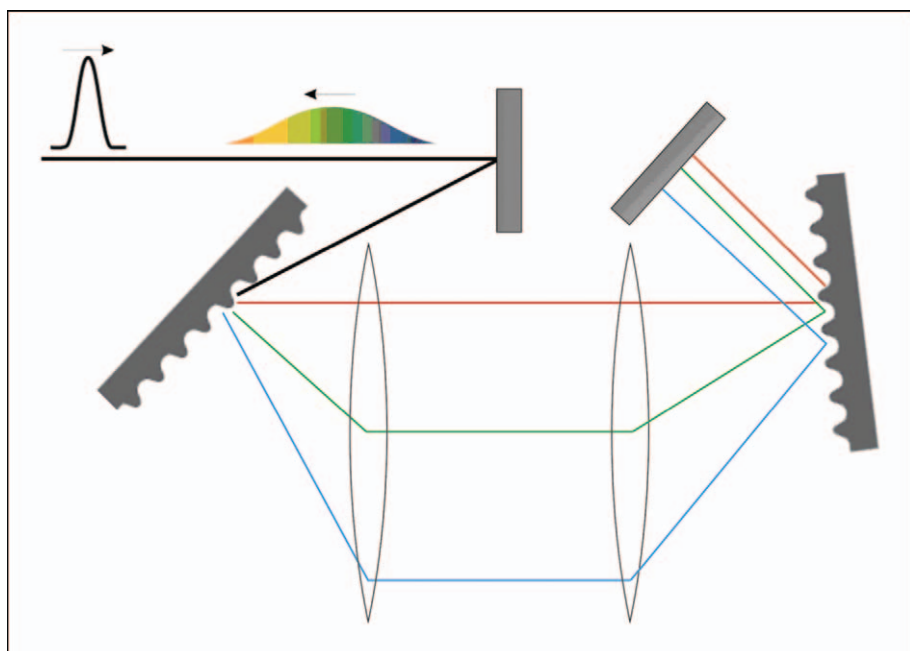
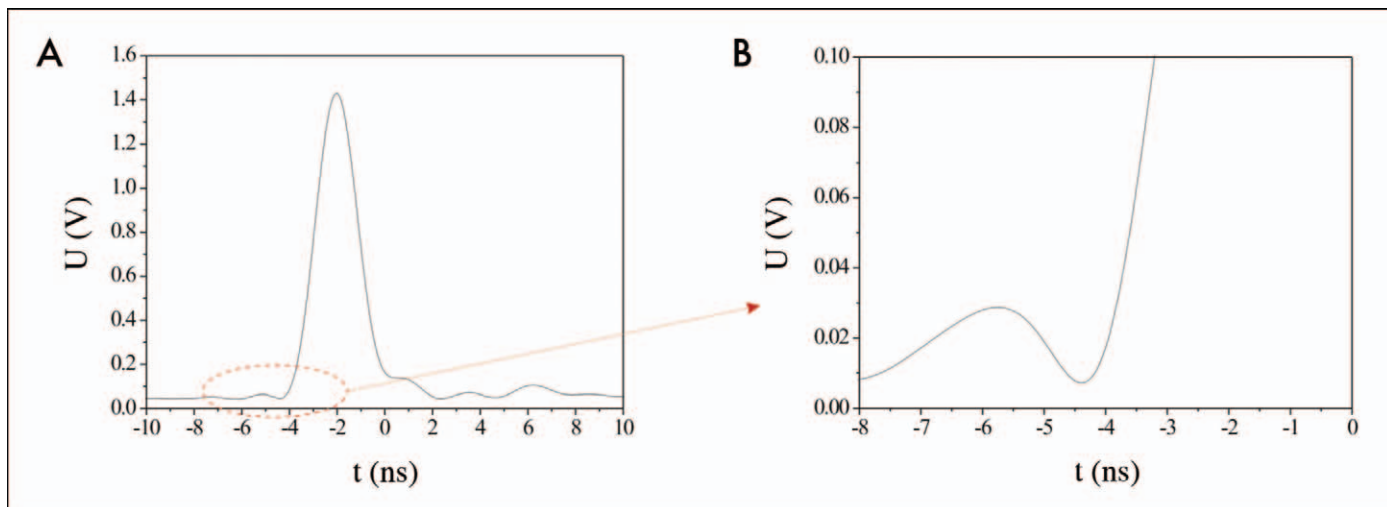


FIG. 3. Principle idea of the stretcher. A femtosecond pulse is converted into a broad chirped pulse.



**FIG. 4.** The fs laser pulse with the pre-pulse measured with a fast photodiode; (a) the main pulse; (b) the pre-pulse. Note that if the laser or the delay of the Pockels cells are not adjusted optimally, the amplitude of the pre-pulse may be worse than 1:100.

to the sample surface (phase front distortion). A 100-fs laser pulse has a pancake shape with a thickness of 30  $\mu\text{m}$  in the direction of propagation. Hence, the adjustment of the sample with respect to the laser beam is important: a 5 mm diameter beam that impacts the sample at an angle of  $10^\circ$ , rather than perpendicularly, interacts with the surface for 3 ps instead of 0.1 ps. A distortion of the pulse front leads to the same effect. This may increase the background and reduce the LIBS signal. Because the length of a nanosecond

laser pulse is roughly 30 cm, which distinctly exceeds the diameter, this effect is negligible for conventional LIBS.

The laser spark is a relatively short event: The plasma and the plasma emission decay in several microseconds or even quicker.<sup>9,21–25</sup> To increase the signal-to-noise ratio, one synchronizes the spectrometer and the laser such that the detector is illuminated only a short time ( $t_{\text{gate}}$ ) after a certain delay ( $t_{\text{delay}}$ ) after the laser pulse. Because the plasma obtained with fs pulses develops dif-

ferently compared to the ns plasma, different delay and gating times are needed for ns- and fs-LIBS.<sup>26</sup>

### STATE-OF-THE-ART IN FEMTOSECOND LASER-INDUCED BREAKDOWN SPECTROSCOPY

Since their discovery in the 1980s, femtosecond lasers have found many different applications in combination with spectrometric techniques but virtually none in analytical science. The first spectrally resolved analysis of a plasma generated by fs laser radiation focused on a target surface was used for purely physical investigation of dense-plasma dynamics rather than for an analytical application.<sup>27</sup> The first reported fs-LIBS application seems to be in real-time process control during laser machining.<sup>28</sup> The first analytical applications of fs-LIBS were reported by Margetic et al.<sup>21</sup> in 2000. Since that time, the number of related publications has grown rapidly.

One of the most important characteristics of an analytical method is the limit of detection (LOD). In the few cases so far measured, the limits of detection for fs-LIBS (see Table I) have been found to be comparable to conventional ns-LIBS. On the other hand, it has been found that accuracy and precision of the sampling

**TABLE I.** Detection limits in fs-LIBS experiments.

Ref.	Laser type and parameters	Spot (mm)	Fluence ( $\text{J}/\text{cm}^2$ )	Element (spectral line, nm)	LOC (ppm)	Delay ( $\mu\text{s}$ )	Gate ( $\mu\text{s}$ )
28	Nd:YAG, 527 nm, 250 fs	0.2	8	Zn (472.2)	4 500	0.5	5
				Cu (465.1)	23 000	0.3	5
25	Ti:Sapphire 800 nm, 100 fs	0.6	20	Cu (324)	3.2	0.5	2.5
				Si (288)	31		
				Ag (388)	1.4	2	5
				Ni (341)	11		
22	Ti:Sapphire 790 nm, 40 fs	0.004	2870	Ca (393.4)	16	?	?
				Ca (396.8)			
8	Ti:Sapphire 800 nm, 100 fs	0.6	20	Mn (403.1)	6.7	1	5
				Mn (404.2)	69		
				Mg (285.2)	2.1		
				Mg (517.3)	25		
				Cu (324.8)	7		
				Cu (521.8)	200		
				Fe (280.0)	22		
				Si (288.2)	80		

are improved considerably.<sup>7,30</sup> This improvement is directly connected to the changes in laser–material interaction. Here, the real benefit of ultra-short laser pulses is apparent: The energy dissipation in the sample material is much more controllable.

The detection limits that have thus far been measured with fs-LIBS are listed in Table I and they show that several ppm can be reached with laser fluences on the order of 10–20 J/cm<sup>2</sup> and a delay between the laser pulse and the spectrometer gate on the order of 1  $\mu$ s. Assion et al.<sup>23</sup> have reported a detection limit for Ca in a CaCl<sub>2</sub> solution in water. The extremely high fluence that they used can be explained by the unexpectedly small spot size reported in the paper. Optimal accumulation times are on the order of several  $\mu$ s. Le Drogoff et al.<sup>26</sup> studied the dependence of the detection limit on delay and gate time. The authors show that for any laser pulse duration (from 80 fs up to 270 ps) there is a corresponding optimal time window providing the best possible detection limit. Remarkably, this LOD is nearly independent of the pulse duration. Femtosecond LIBS has been applied for brass and aluminum alloys to address the issue of fractionation.<sup>9,21</sup> It has been found that due to the special ablation mechanism (i.e., energy confinement) fractionation is minimized.

Beside these conventional applications of fs lasers in LIBS, several investigations have addressed new possibilities. A proposed application that has been tested successfully is in-depth profiling.<sup>31</sup> Similarly, femtosecond laser ablation was used for process control and diagnostics in micromachining of sandwiched structures. The achievable processing precision of femtosecond lasers is supported by precise endpoint detection using spectrometric means.<sup>32</sup> In both cases, minimal heat-induced collateral damage in the fs laser ablation process, is observed.

Similarly, fs-LIBS has been used for analyzing biological samples with high spatial resolution. However, here the idea is that the efficient

use of the delivered energy minimizes collateral damage induced by the mechanical shock wave instead of heat-induced damages.<sup>30</sup>

To improve spatial resolution, the size of the probed volume can be even further decreased by the application of near-field techniques.<sup>33,34</sup> Hypothetically, a combination of fs-LIBS with *near field ablation* allows a significant decrease in the crater diameter to far below the wavelength-limited far field boundary, e.g., approaching 100 nm and below. It has already been demonstrated that a 600 nm crater can be produced with a 775 nm IR laser in this way.<sup>34</sup> The foundation of this new possibility lies in the lower ablation thresholds of femtosecond-induced material removal.<sup>35,36</sup> Ablation thresholds are considerably lowered because of the more efficient use of the energy that is delivered.

In order to improve detection limits, double pulses in different configurations have been applied. This can also be done with a combination of nanosecond and femtosecond pulses. Scaffidi et al.<sup>37</sup> have studied the spectrum intensity for different time delays between the collinear fs and ns pulses as well as for different distances between the sample surface and the laser focus. In Ref. 38 an orthogonal alignment of the femtosecond and a nanosecond pulses was studied. The experiments demonstrated an increase in the fs-LIBS signal if the femtosecond impulse is followed by a reheating nanosecond laser-induced plasma, which reheats the plasma ablated in the femtosecond pulse and thereby changes the pressure conditions of the ablation. Compared to a single pulse in the same experimental setup, an improvement of the LOD by approximately a factor of 10 was achieved.<sup>29</sup>

The idea of the double-pulse experiment is similar to the idea of temporal pulse shaping.<sup>25</sup> Here, the pulse is temporally shaped in a setup similar to the previously described stretcher.<sup>39</sup> For the same reason, one can combine the effect of up- or down-chirping<sup>40</sup> or pulse-shaping in

the spatial domain,<sup>33</sup> with femtosecond LIBS measurements.

One of the most remarkable features of LIBS is the possibility of performing a measurement at a distance without contacting the sample directly. This is generally referred to as stand-off or *remote LIBS*. An important characteristic of this technique is the maximal distance at which the measurement can be carried out. One of the limiting factors to this distance is the laser beam divergence, which can be overcome by *self-focusing* or *self-trapping*.<sup>16,17</sup> If the beam power is high enough, the beam propagates in a self-induced waveguide in the air. The higher peak power of the femtosecond lasers promotes this effect. The self-focusing allows one to use fs-LIBS for remote analysis of dangerous samples or samples that cannot be transported to the laboratory.<sup>20,41,42</sup> It is important for ecological applications, remote detection of explosives, toxic, and radioactive materials, or for cultural heritage work.<sup>35,43–45</sup>

To summarize this section, it can be concluded that fs laser ablation opens up new, special applications for LIBS such as (1) high resolution, topographic profiling (lateral, in-depth), (2) analysis of biological, explosive, and brittle samples, and (3) remote analysis.

These applications are special in the sense that their success relies on a very specific laser–material interaction that only occurs with fs lasers. In the following section we will discuss the peculiarities in the physical mechanism that make fs lasers especially well suited for these applications. Further possible future applications that may lie in the realm of fs lasers will be discussed in the Conclusion.

## LASER–MATERIAL INTERACTION

Depending on the material, different ablation mechanisms have been proposed. At the irradiances usually applied for femtosecond LIBS (see Table I), which exceed 10<sup>13</sup> W/cm<sup>2</sup>, most of the relevant physics can be understood in the framework of ther-

mal ablation. Only in special applications (e.g., near-field ablation) at fluences close to the ablation threshold do other mechanisms become relevant. According to Rethfeld et al.,<sup>46</sup> the ablation mechanism of dielectrics and semiconductors should be considered as non-thermal melting or as a direct transition into the plasma state. Other possible mechanisms such as Coulomb explosion, spallation, and others may also exist.<sup>47,48</sup>

At the wavelength range considered, absorption can only be mediated by electrons. Due to a lack of free charge carriers, the first step in the ablation of non-metal samples (insulators and wide-band semiconductors) is the creation of such electrons. Although the photon energy is less than the band-gap width and one photon is unable to ionize, a high photon density in the laser radiation may suffice. A complex mechanism of multiphoton-assisted avalanche breakdown is responsible for the free-carrier generation and the breakdown of the material in ultra-short pulse ablation.<sup>49,50</sup> This is in contrast to ns to second ablation in which a random first electron must already exist to start the avalanche. Based on the self-seeding process, the improvement in shot-to-shot repeatability is understandable.

The improvement provided by fs lasers can be easily understood: In the first step, an electron from the valence band absorbs a photon and increases its energy, which now corresponds to a value in the gap between the valence and conduction zones. Most probably, there are no energy levels in the gap and the electron must decay to the initial energetic state and reemit the absorbed photon. However, photo-ionization is not an instantaneous process. It lasts about a femtosecond due to the uncertainty relation. For an energy variation of 1 eV, we have:  $t_i \sim h/E_0 \sim 10^{-15}$  s. Consequently, simultaneous absorption means absorption in  $10^{-15}$  s (a more accurate estimation by Raizer<sup>24</sup> gives a similar result). If the photon flux density is strong enough, after several jumps the photon reach-

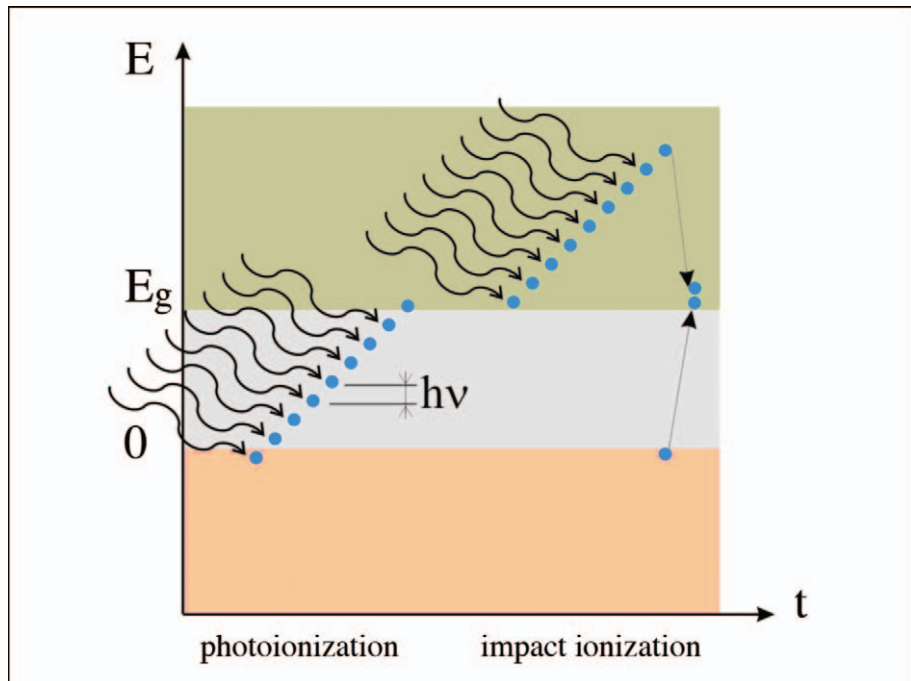


**FIG. 5.** Schematic representation of (left) multiphoton ionization and (right) impact ionization in insulators or semiconductors where the band gap  $E_g$  exceeds the photon energy  $h\nu$ .

es the conduction band (see Fig. 5, left). A simple estimation demonstrates the possibility of this mechanism, especially for an ultra-short laser pulse: A 1 mJ, 100 fs laser field focused in a 50  $\mu\text{m}$  spot produces such a strong photon flux that in 1 fs a surface of 1  $\text{\AA}^2$  is irradiated by roughly one thousand photons. Note that normally only ten photons are needed for photo-ionization with an IR laser pulse.

In the second step, an electron in the conduction band can absorb photons and increase its own kinetic energy in this way. After several absorption events, the energy of the electron exceeds the band gap width and impact ionization becomes possible. In this way the electron density doubles and an electron avalanche develops, shown in Fig. 5, right.

As already motioned, in certain situations the assistance of an avalanche by multiphoton seeding is especially advantageous. This occurs if not enough free electrons are available, since in this case the fs pulses are accompanied by a gain in shot-to-shot stability,<sup>7,51</sup> or if the delivered

photon number needs to be as low as possible. These situations arise if (1) pure, transparent material is analyzed, high spatial resolution on transparent samples is necessary, or near-field ablation is used; or (2) in-depth analysis with high resolution is required.

In the first two cases the random electron that triggers the avalanche may not exist. In the other two cases, the photon number is low due to the limited transport efficiency of the sub-wavelength aperture or due to low fluences used to improve the attainable depth resolution.

Shortly after the sample illumination starts, the surface layer of an insulator has reached an electron density comparable to that of a metal. Hence, in the following, only laser-metal interactions will be discussed. The fundamental interaction of ultra-short laser pulses with materials can be understood directly from a two-temperature model.<sup>5</sup> The radiation can only heat one component of the sample: the electrons that are close to the surface absorb the laser radiation and subsequently thermalize on

a time-scale of  $10^{-13}$  s.<sup>52,53</sup> The electron equilibrium temperature is between 1 and 100 eV.<sup>52</sup> The ions, on the other hand, remain at room temperature.

The hot electrons transfer their energy to the lattice via electron-phonon interactions (thermal melting).<sup>46,55</sup> The lattice melts within a few picoseconds after the laser irradiation starts and the ablation takes place. Here, it is speculated that homogenous melting (phase explosion) sometimes takes place. However, it appears that most effects can be explained by surface evaporation.<sup>5,6,48</sup> It is this rapid removal of material which basically results in a confinement of the delivered energy to the region that is removed. The heat load to the surrounding material, which results in fractionation, phase-boundary distortion, and other collateral damage, is thereby minimized.

The thermal scenario dominates for ns and ps laser ablation; non-thermal behavior can be achieved in semiconductor and dielectric samples with fs lasers. An overview of the time scales for the laser-solids interaction is shown in Fig. 6 and can be found in Rethfeld et al.<sup>46</sup> Here a remarkable difference between the femtosecond and a pico- or nanosecond laser ablation can be seen: there is no ablated material above the surface until the end of the femtosecond laser pulse. This makes the ablation easier and allows a dense ablated plasma to be formed with a higher efficiency than with longer pulses, which are partly screened by the ablated material.

The different peak power and duration of the laser influences the ablation crater as well. The time scale of the nanosecond ablation is comparable with the heat diffusion times. Hence, it is accompanied by a temperature wave propagating into the bulk of the sample. This heating melts the target near the irradiated spot. The shock wave propagating through the melt layer and the ablation-induced reactive force press the melt out of the crater and initiate splashing of the liquid material. It

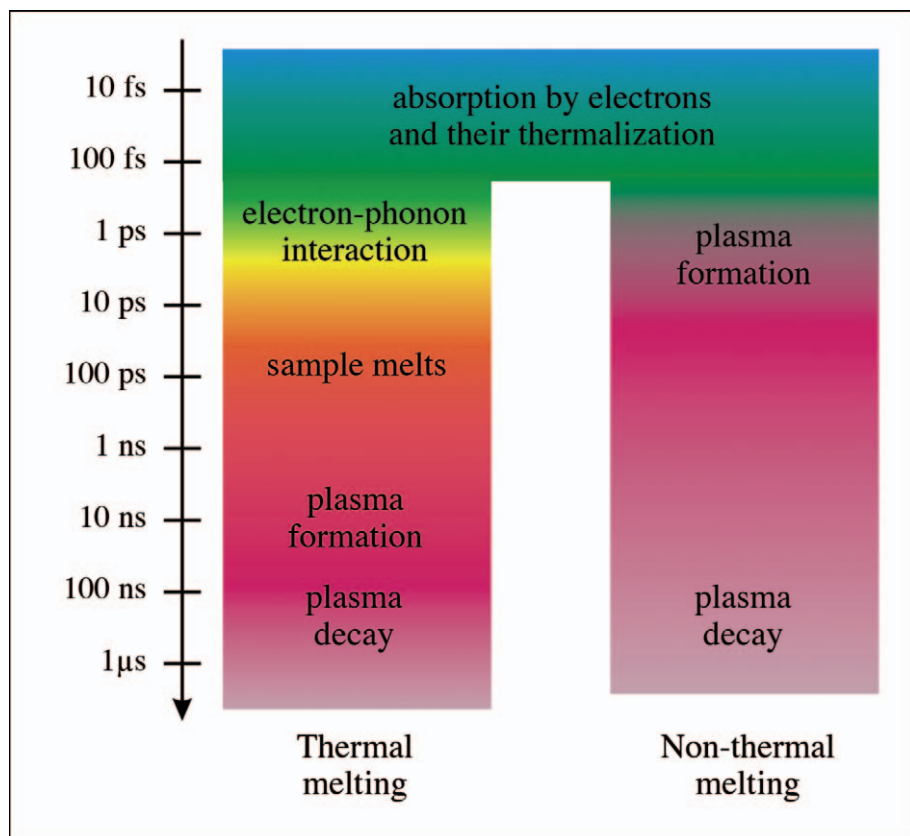


FIG. 6. An overview of the time scales for the laser-solids interaction.

then solidifies, forming a rim around the ablated area, as seen in Fig. 7b. On the other hand, femtosecond ablation provides a quick evaporation of the hot material and prevents or reduces the formation of the melt layer. The resulting crater has no resolidified melt edge common in the thermal case. The different crater shapes have been reported by many authors, see e.g., Refs. 21, 30, 56, and 57.

Femtosecond LIBS measurements are confined to a relatively thin surface layer of the sample because only 10–100 nm is ablated in each shot. Such a small ablation depth per pulse opens the possibility for depth-profiling and analysis of multi-layer samples.<sup>31,58</sup> An important condition here is a well-defined flat crater shape and a minimal formation of the melt layer in the crater: the melt layer may decrease the depth resolution due to possible formation of an alloy consisting of materials corresponding to different layers. A

non-flat crater profile leads to simultaneous ablation of different depths in one shot. As already mentioned, the heat-affected zone is reduced by femtosecond ablation, which can be easily seen from the shape of the crater shown in Fig. 7. This difference is also important for analytical applications, especially for calibration and mapping with good spatial resolution.

## THE LASER PLASMA

Up to now all experimental evidence shows that the average optical emission characteristics of the ablation plasma created by a fs laser under atmospheric conditions differ very little from those of conventional LIBS plasmas. Whereas in ns-pulse-created plasmas the luminance increases in the first 100 ns after the laser pulse, the fs-pulse-created plasma ceases after a very short time ( $t > 1$  ns). This corresponds to the bremsstrahlung background, which

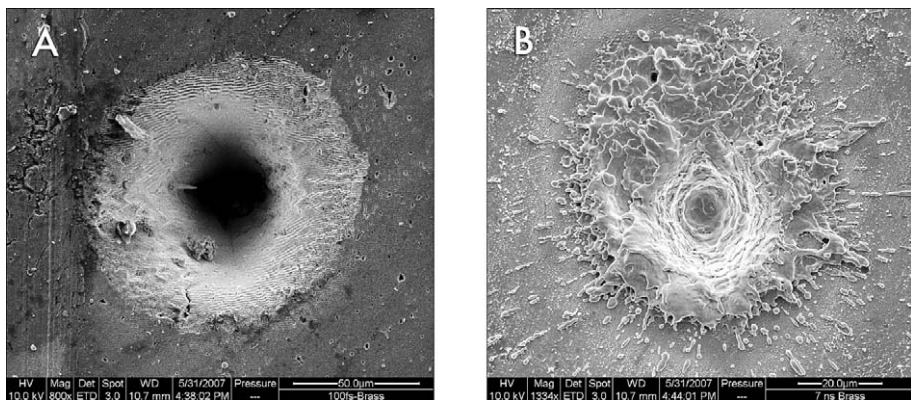


**Fig. 7.** A crater made in a brass sample by (a) 100 fs laser pulses and (b) 7 ns laser pulses in air at atmospheric pressure.

is found to be far lower and of shorter duration ( $<5$  ns, see Ref. 59) in the ultra-short pulse case. This effect is explained by the direct heating of the expanding plasma by the trailing part of the ns laser pulse via electron-neutral, electron-ion bremsstrahlung and photoionization of the plasma and the ambient gas. However, the effect only becomes noticeable for pulse durations in excess of several picoseconds. This heating also explains the higher electron temperature and density, which lead to the emission of a broad bremsstrahlung spectrum and to the broadening of the spectral lines often observed by the nanosecond laser-induced plasmas but not seen in fs laser-induced plasmas created under typical LIBS conditions.<sup>9</sup>

Clear differences are found between the hydrodynamic expansion of femtosecond and nanosecond laser-generated plasma.<sup>21,60–62</sup> At early times, the expansion of the fs-laser-produced plasma is much stronger in the direction normal to the surface relative to the perpendicular. Considering the pressure confinement due to strong overheating in the laser impact zone, the one-dimensional expansion is understandable. At later times the expansion is approximated by a blast wave and assuming adiabatic expansion, the plasma radius  $R$  is proportional to the cube root of the absorbed laser energy. In comparison to laser plumes produced by ns laser pulses, this relation holds well over a wide range of parameters,

which is understandable if the time scale of energy deliverance to the sample ( $<1$  ps) is compared to the plasma expansion regime ( $>1$   $\mu$ s).

Gas breakdown is characterized by the breakdown threshold, which is the irradiance ( $W\text{ cm}^{-2}$ ) or electric field, at which breakdown occurs. Theory and experiments show that the irradiance for the breakdown threshold is proportional to  $\tau_p^{-1/2}$ , i.e., it is higher for femtosecond laser radiation than for nanosecond laser radiation.<sup>36,63</sup> Hence, breakdown in a gaseous environment is less probable for fs lasers than for ps or ns lasers of the same power. But on the other hand, the power of fs lasers is normally several orders of magnitude higher and this higher threshold can be easily overcome.

If the laser field intensity in the ambient atmosphere is high enough, optical breakdown may take place. If so, a considerable part of the laser energy is expended on the ionization and is absorbed by the plasma that is formed. This unwelcome effect also leads to the appearance of spectral lines due to species that compose the ambient gas. It was demonstrated by Rohwetter et al.<sup>42</sup> that LIBS spectra of metallic samples measured in air with a picosecond laser contain oxygen and nitrogen spectral lines, which are not observed with a femtosecond laser. However, as already mentioned, in some cases the optical breakdown can be favorably used for spectroscopic applications, as in self-focusing for remote LIBS. Self-focusing

is the formation of a self-induced waveguide in the atmospheric air.<sup>15,16</sup> It enables one to deliver a high-intensity laser beam at a distance of a hundred meters or more for remote LIBS.<sup>20,41</sup>

## CONCLUSION

Current achievements in femtosecond LIBS, which is a new, promising tool for surface diagnostics, have been reviewed. Information gathered up to now shows that a real breakthrough in terms of better LOD cannot be expected. However, in some cases precision and accuracy are improved because the onset of ablation is basically self-triggered due to multiphoton absorption. Additionally, melting, as a source of possible fractionation effects, is significantly reduced. Indeed, inductively coupled plasma mass spectrometry (ICP-MS) measurements, which are hampered by similar problems, demonstrate fewer matrix effects by the use of femtosecond instead of nanosecond ablation. Hopefully this result can be transferred to LIBS as well.

As with nanosecond laser LIBS, the quality and dynamics of fs-LIBS spectra depend on many factors such as spectrometer gating, surrounding gas pressure, position of the laser focus, and other factors. The optimal experimental parameters for various fs-LIBS implementations have not yet been found; thus, there is a large need for methodical experimental optimization. However, based on the underlying physics, new fields of application for LIBS have been identified and discussed. Compared to conventional LIBS, these applications of femtosecond lasers have the following features:

- higher laser peak power combined with minimized energy dissipation in the sample results in lower ablation thresholds ( $J\text{ cm}^{-2}$ )
- more effective ablation due to energy confinement
- less sample heating and damage
- fewer matrix effects in the ablation process
- well-defined crater shape

- higher shot-to-shot stability
- beam filamentation for remote LIBS
- better spatial resolution for surface mapping

These applications are based on the more precise control of the delivered energy due to energy confinement and the short interaction time of the removed and retained material. The goal would be gathering topochemical information with high resolution or the analysis of fragile material such as biological samples, explosives, and brittle materials (e.g., powders). The spatial resolution of the method can be further improved by combining the fs-LIBS with near-field ablation techniques.

Another possible unexplored starting point for new applications of ultra-short laser pulses is, paradoxically, the possibility of lengthening the pulse duration in order to take advantage of a broad spectral range. Dual-pulse experiments, the effect of up- or down-chirping, or recent experiments—not directly related to LIBS—with temporal pulse shaping all indicate that the control of energy flux may improve ablation or open up new directions.

A further decrease of the laser pulse duration seems to be unlikely because attosecond pulses cannot be generated in visible light. Indeed, a physical limit of a few field cycles has already been reached in the IR and visible parts of the spectrum. A shorter pulse is possible only in the XUV or in the X-ray range. This is problematic from the technical point of view.

Femtosecond LIBS is a new analytical method based on femtosecond laser techniques. The physical processes of the femtosecond ablation and plasma formation are not completely understood. Effective optimization of the LIBS instrumentation and parameters is hardly possible without a detailed understanding of this underlying physics. This is a nice example of direct application of frontier physics in industry because the solution of many industrial and analytical tasks can be improved by introducing fs-LIBS as documented

by a growing number of publications and conference contributions devoted to this subject.

1. K. Song, Y.-I. Lee, and J. Sneddon, *Appl. Spectrosc. Rev.* **37**, 89 (2002).
2. A. W. Miziolek, V. Palleschi, and I. Schechter, Eds., *Laser-Induced Breakdown Spectroscopy (LIBS). Fundamentals and Applications* (Cambridge University Press, New York, 2006).
3. D. A. Cremers and L. J. Radziemski, *Handbook of Laser-Induced Breakdown Spectroscopy* (John Wiley and Sons, New York, 2006).
4. W. Demtröder, *Laser Spectroscopy. Basic Concepts and Instrumentation* (Springer, Berlin, 2003).
5. B. N. Chichkov, C. Momma, S. Nolte, F. von Alvensleben, and A. Tuennermann, *Appl. Phys. A* **63**, 109 (1996).
6. D. von der Linde, K. Sokolowski-Tinten, and J. Bialkowski, *Appl. Surf. Sci.* **110**, 1 (1997).
7. R. E. Russo, X. L. Mao, C. Liu, and J. Gonzalez, *J. Anal. At. Spectrom.* **19**, 1084 (2004).
8. F. Dausinger, F. Lichtner, and H. Lubatschowski, *Femtosecond Technology for Technical and Medical Applications* (Springer, Berlin, 2004).
9. B. Le Drogoff, J. Margot, M. Chaker, M. Sabsabi, O. Barthélemy, T. W. Johnston, S. Laville, F. Vidal, and Y. von Kaenel, *Spectrochim. Acta, Part B* **56**, 987 (2001).
10. B. Le Drogoff, J. Margot, F. Vidal, S. Laville, M. Chaker, M. Sabsabi, T. W. Johnston, and O. Barthélemy, *Plasma Sources Sci. Technol.* **13**, 223 (2004).
11. D. Strickland and G. Mourou, *Opt. Commun.* **56**, 219 (1985).
12. T. Brabec and F. Krausz, *Rev. Mod. Phys.* **72**, 545 (2000).
13. V. V. Semak, B. R. Campbell, and J. G. Thomas, *J. Phys. D: Appl. Phys.* **39**, 3440 (2006).
14. G. A. Askarjan, *Sov. Phys. JETP* **15**, 1088 (1962).
15. R. Y. Chiao, R. Garmire, and C. H. Townes, *Phys. Rev. Lett.* **13**, 479 (1964).
16. L. Berg, S. Skupin, F. Lederer, G. Méjean, J. Yu, J. Kasparian, E. Salmon, J. P. Wolf, M. Rodriguez, L. Wöste, R. Bourayou, and R. Sauerbrey, *Phys. Rev. Lett.* **92**, 225002 (2004).
17. E. Yablonovitch, *Phys. Rev. Lett.* **31**, 877 (1973).
18. R. G. Brewer, *Phys. Rev. Lett.* **19**, 8 (1967).
19. W. M. Wood, C. W. Siders, and M. C. Downer, *Phys. Rev. Lett.* **67**, 3523 (1991).
20. K. Stelmasczyk, P. Rohwetter, G. Méjean, J. Yu, E. Salmon, J. Kasparian, R. Ackermann, and J. P. Wolf, *Appl. Phys. Lett.* **85**, 3977 (2004).
21. V. Margetic, A. Pakulev, A. Stockhaus, M. Bolshov, K. Niemax, and R. Hergenröder, *Spectrochim. Acta, Part B* **55**, 1771 (2000).
22. O. Albert, S. Roger, Y. Glinec, J. C. Loughere, J. Etchepare, C. Boulmer-leborgne, J. Perrière, and E. Millon, *Appl. Phys. A* **76**, 319 (2003).
23. A. Assion, M. Wollenhaupt, L. Haag, F. Mayorov, C. Sarpe-Tudoran, M. Winter, U. Kutschera, and T. Baumert, *Appl. Phys. B* **77**, 391 (2003).
24. Y. P. Raizer, *Sov. Phys. Uspekhi* **8**, 650 (1966).
25. V. Hommes, M. Miclea, and R. Hergenröder, *Appl. Surf. Sci.* **252**, 7449 (2006).
26. B. Le Drogoff, M. Chaker, J. Margot, M. Sabsabi, P. Barthélemy, T. W. Johnston, S. Laville, and F. Vidal, *Appl. Spectrosc.* **58**, 122 (2004).
27. J. A. Cobble, G. A. Kyrala, A. A. Hauer, A. J. Taylor, C. C. Gomez, N. D. Delamater, and G. T. Schappert, *Phys. Rev. A* **39**, 454 (1989).
28. B. M. Kim, M. D. Feit, A. M. Rubenchik, B. M. Mammini, and L. B. D. Silva, *Appl. Surf. Sci.* **127**, 857 (1998).
29. A. Santagata, A. De Bonis, P. Villani, R. Teghil, and P. G. Parisi, *Appl. Surf. Sci.* **252**, 4685 (2006).
30. O. Samek, V. Margetic, and R. Hergenröder, *Anal. Bioanal. Chem.* **381**, 54 (2005).
31. V. Margetic, M. Bolshov, A. Stockhaus, K. Niemax, and R. Hergenröder, *J. Anal. At. Spectrom.* **16**, 616 (2001).
32. T. Tong, J. Li, and J. P. Longtin, *Appl. Opt.* **43**, 1971 (2004).
33. O. Samek, V. Hommes, and R. Hergenröder, *Rev. Sci. Instrum.* **76**, 086104 (2005).
34. O. Samek, A. Kurowski, S. Kittel, S. V. Kulklevsky, and R. Hergenröder, *Spectrochim. Acta, Part B* **60**, 1225 (2005).
35. M. D. Perry, B. C. Stuart, P. S. Banks, M. D. Feit, V. Yanovsky, and A. M. Rubenchik, *J. Appl. Phys.* **85**, 6803 (1999).
36. M. H. Niemi, *Appl. Phys. Lett.* **66**, 1181 (1995).
37. J. Scaffidi, W. Pearman, J. C. Carter, and S. M. Angel, *Appl. Spectrosc.* **60**, 65 (2006).
38. J. Scaffidi, J. Pender, W. Pearman, S. R. Goode, B. W. Colston, Jr., J. C. Carter, and S. M. Angel, *Appl. Opt.* **42**, 6099 (2003).
39. A. M. Weiner, *Rev. Sci. Instrum.* **71**, 1929 (2000).
40. T. Gunaratne, M. Kangas, S. Singh, A. Gross, and M. Dantus, *Chem. Phys. Lett.* **423**, 197 (2006).
41. P. Rohwetter, K. Stelmasczyk, L. Wöste, R. Ackermann, G. Mejean, E. Salmon, J. Kasparian, J. Yu, and J. P. Wolf, *Spectrochim. Acta, Part B* **60**, 1025 (2005).
42. P. Rohwetter, W. Yu, G. Méjean, K. Stelmasczyk, E. Salmon, J. Kasparian, J. P. Wolf, and L. Wöste, *J. Anal. At. Spectrom.* **19**, 437 (2004).
43. T. Fujii, N. Goto, K. Sugiyama, M. Miki, T. Nayuki, K. Nakajima, and K. Nemoto, in *LIBS 2006 Laser Induced Plasma Spectroscopy and Applications* (Montreal, Canada, September 5–8, 2006).
44. S. Tzortzakis, D. Anglos, and D. Gray, *Opt. Lett.* **31**, 1139 (2006).

45. Q. Luo, H. L. Xu, S. A. Hosseini, J. F. Daigle, F. Théberge, M. Sharifi, and S. L. Chin, *Appl. Phys. B* **80**, 105 (2006).
46. B. Rethfeld, K. Sokolowski-Tinten, D. Von der Linde, and S. I. Anisimov, *Appl. Phys. A* **79**, 767 (2004).
47. D. Perez and L. J. Lewis, *Phys. Rev. Lett.* **89**, 255504 (2002).
48. D. Perez and L. J. Lewis, *Phys. Rev. B* **67**, 184102 (2003).
49. S. S. Mao, F. Quéré, S. Guizard, X. Mao, R. E. Russo, G. Petite, and P. Martin, *Appl. Phys. A* **79**, 1695 (2004).
50. F. Rossi and T. Kuhn, *Rev. Mod. Phys.* **74**, 895 (2002).
51. R. Hergenröder, O. Samek, and V. Hommes, *Mass Spectrosc. Rev.* **25**, 551 (2006).
52. J. R. Goldman and J. A. Prybyla, *Phys. Rev. Lett.* **72**, 1364 (1994).
53. W. H. Knox, C. Hirlimann, D. A. B. Miller, J. Shah, D. S. Chemla, and C. V. Shank, *Phys. Rev. Lett.* **56**, 1191 (1986).
54. D. V. Fisher, Z. Henis, S. Eliezer, and J. Meyer-Ter-Vehn, *Laser Particle Beams* **24**, 81 (2006).
55. K. Sokolowski-Tinten, J. Bialkowski, M. Boing, A. Cavalleri, and D. von der Linde, *Phys. Rev. B* **58**, R11805 (1998).
56. J. H. Yoo, S. H. Jeong, G. Greif, and R. E. Russo, *J. Appl. Phys.* **88**, 1638 (2000).
57. C. Liu, X. L. Mao, S. S. Mao, X. Zeng, R. Greif, and R. E. Russo, *Anal. Chem.* **76**, 379 (2004).
58. M. P. Mateo, G. Nicolas, V. Pinon, and A. Yanez, *Surf. Interface Anal.* **38**, 941 (2006).
59. S. Yalcin, Y. Y. Tsui, and R. Fedosejevs, *J. Anal. At. Spectrom.* **19**, 1295 (2004).
60. X. Zeng, X. L. Mao, R. Greif, and R. E. Russo, *Appl. Phys. A* **80**, 237 (2005).
61. V. Margetic, T. Ban, E. Leis, K. Niemax, and R. Hergenröder, *Spectrochim. Acta, Part B* **58**, 415 (2003).
62. V. Margetic, T. Ban, O. Samek, F. Leis, K. Niemax, and R. Hergenröder, *Czech. J. Phys.* **54**, 423 (2004).
63. C. L. M. Ireland, *J. Phys. D: Appl. Phys.* **7**, L179 (1974).